

Utilizing magnetic resonance imaging (MRI) to assess the effects of angling-induced barotrauma on rockfish (*Sebastes*)

Bonnie L. Rogers, Christopher G. Lowe, Esteban Fernández-Juricic, and Lawrence R. Frank

Abstract: The physical consequences of barotrauma on the economically important rockfish (*Sebastes*) were evaluated with a novel method using T_2 -weighted magnetic resonance imaging (MRI) in combination with image segmentation and analysis. For this pilot study, two fishes were captured on hook-and-line from 100 m, euthanized, and scanned in a 3 Tesla human MRI scanner. Analyses were made on each fish, one exhibiting swim bladder overinflation and exophthalmia and the other showing low to moderate swim bladder overinflation. Air space volumes in the body were quantified using image segmentation techniques that allow definition of individual anatomical regions in the three-dimensional MRIs. The individual exhibiting the most severe signs of barotrauma revealed the first observation of a gas-filled orbital space behind the eyes, which was not observable by gross dissection. Severe exophthalmia resulted in extreme stretching of the optic nerves, which was clearly validated with dissections and not seen in the other individual. Expanding gas from swim bladder overinflation must leak from the swim bladder, rupture the peritoneum, and enter the cranium. This MRI method of evaluating rockfish following rapid decompression is useful for quantifying the magnitude of internal barotrauma associated with decompression and complementing studies on the effects of capture and discard mortality of rockfishes.

Résumé : Nous avons évalué les conséquences physiques des barotraumatismes sur les sébastes du genre *Sebastes*, des poissons d'importance économique, à l'aide d'une méthode inédite utilisant l'imagerie par résonance magnétique (MRI) pondérée en T_2 en combinaison avec la segmentation et l'analyse des images. Dans cette étude pilote, nous avons capturé deux poissons à la ligne à une profondeur de 100 m et les avons euthanasiés et analysés dans un scanner à 3 teslas pour humains. Les analyses faites chez les deux poissons montrent, chez l'un, une inflation excessive de la vessie natatoire et une exophthalmie et, chez l'autre, une inflation excessive faible à modérée de la vessie natatoire. Nous avons mesuré les volumes des espaces aériens dans le corps par des techniques de segmentation des images qui permettent une définition des diverses régions anatomiques en MRI 3D. L'individu qui présente les symptômes les plus importants de barotraumatisme possède un espace orbital rempli de gaz derrière les yeux qui n'est pas visible à la dissection grossière. L'exophthalmie sévère cause un étirement extrême des nerfs optiques qui se vérifie clairement à la dissection et qui n'est pas visible chez l'autre individu. Le gaz en expansion provenant de l'inflation excessive de la vessie natatoire doit s'échapper de la vessie, fendre le péritoine et s'infiltrer dans le crâne. Notre méthode d'évaluation des sébastes par MRI après une décompression rapide est utile pour mesurer l'importance du barotraumatisme interne associé à la décompression et elle sert de complément aux études des effets de la capture et de la mortalité reliée à la remise à l'eau chez les sébastes.

[Traduit par la Rédaction]

Introduction

In the eastern Pacific, rockfish (*Sebastes* spp.) comprise one of the most important and economically valuable

groundfish. Many rockfish populations are declining as a result of high discard mortality and overexploitation (Davis 2002; Parker et al. 2006). High discard mortality of physoclistic fishes has been attributed to barotrauma on the fish resulting in swim bladder overinflation and rupture,

Received 18 December 2007. Accepted 22 April 2008. Published on the NRC Research Press Web site at cjfas.nrc.ca on 15 May 2008. J20329

B.L. Rogers,¹ C.G. Lowe, and E. Fernández-Juricic. Department of Biological Sciences, California State University Long Beach, 1250 Bellflower Boulevard, Long Beach, CA 90840, USA.

L.R. Frank. Center for Scientific Computation in Imaging and Center for Functional MRI, University of California San Diego, La Jolla, CA 92037, USA.

¹Corresponding author (e-mail: brogers2@csulb.edu).

exophthalmia (eye protrusion), and prolapsed stomach and (or) cloacae (Wilson and Burns 1996; Nichol and Chilton 2006; Hannah and Matteson 2007). The number and degree of visible trauma symptoms in rockfish (*Sebastes* spp.) are highly variable among individuals and species and not a good predictor of survival (Jarvis and Lowe 2008). Knowledge of internal damage associated with barotrauma is limited, and more empirical evidence quantifying morphological and physical damage is needed. Thus far, methods quantifying damage in rockfish have been limited purely to visual inspection.

In red snapper (*Lutjanus campechnus*), two-dimensional X rays revealed a pattern of increasing organ displacement following decompression (Rummer and Bennett 2005), but volumes were estimated by measuring organ dimensions, which is subject to error. Magnetic resonance imaging (MRI), on the other hand, provides a fully three-dimensional (3D) digital image from which any fish organ dimension can be measured accurately (in cubic millimetres). Although X rays create contrast based on bone density, MRI has an advantage of visualizing and depicting soft tissues based on water content. For example, T_1 -weighted MRI scanning on the shortfin mako shark (*Isurus oxyrinchus*) and the salmon shark (*Lamna ditropis*) allowed quantification of red muscle that provided precise and unique detail about the position, volume, and types of red muscle (Perry et al. 2007). MRI methodology can reveal internal tissue and organ placement, and displacement, immediately following trauma and specifically display which areas are composed of tissue or gas.

The goals of this study using MRI were (i) to characterize the morphological changes of the internal organs and ocular-orbital regions in rapidly decompressed rockfish using MRI techniques and (ii) to determine whether this technique could be used as a diagnostic tool for assessing and characterizing internal injury resulting from fishing-related barotrauma. Because of the high cost of MRI operations, only two rockfish were surveyed as part of this “proof of concept” study. We quantified the relative magnitude of differences between a fish exhibiting many signs of internal barotrauma and one showing few signs.

Materials and methods

Two rockfish, one honeycomb (*Sebastes umbrosus*) and one greenblotched (*Sebastes rosenblatti*), were caught using hook-and-line off the coast of Long Beach, California (Potter's Reef) from a depth of 100 m at seafloor, euthanized, and transported in an ice-bath slurry to the MRI facility. The two species have very similar body morphologies, belong to overlapping and homologous ecotypes, and inhabit boulder fields or other rocky bottoms (Love et al. 2002). Although there are likely interspecific differences in morphology and physiology, the goals of this study were to determine whether MRI techniques could be used to quantify internal morphological damage and volume spaces caused by barotrauma.

The honeycomb rockfish (fish with visible trauma (fish VT); 18 cm standard length (SL)) showed visible external signs of barotrauma, including exophthalmia and corneal gas in both eyes, stomach eversion, and an overinflated

swim bladder evident by an extremely swollen abdomen. The greenblotched rockfish (fish with no visible trauma (fish NVT); 22 cm SL) showed little external signs of barotrauma, no visible eye trauma, and an overinflated swim bladder visible by a moderately swollen abdomen, although this fish was also rapidly decompressed. Four hours after being caught, both fish were euthanized with an overdose of tricaine methanesulfonate (MS 222) and placed one at a time inside a magnetic resonance imaging (MRI) unit for whole-body scanning. Photographs taken of the fish just after capture and again after MRI imaging indicated little change in physical appearance.

Images were acquired on a 3 Tesla (3T) GE SIGNA clinical imaging system using an eight-channel head array coil (MRI Devices, Waukesha, Wisconsin). Two data image sets were acquired for each specimen, a T_1 -weighted sequence and a T_2 -weighted sequence. Total imaging time was 2 h for both fish (30 min-scan⁻¹). The T_1 -weighted sequence of a fast RF-spoiled gradient recalled echo (FSPGR) produces high contrast between different tissue types, whereas the T_2 -weighted sequence was a steady-state free precession (SSFP) method that produces high contrast between tissues and fluids. The T_2 -weighted images produced better contrast near the eye regions and were the only scans used for the image analyses in this study.

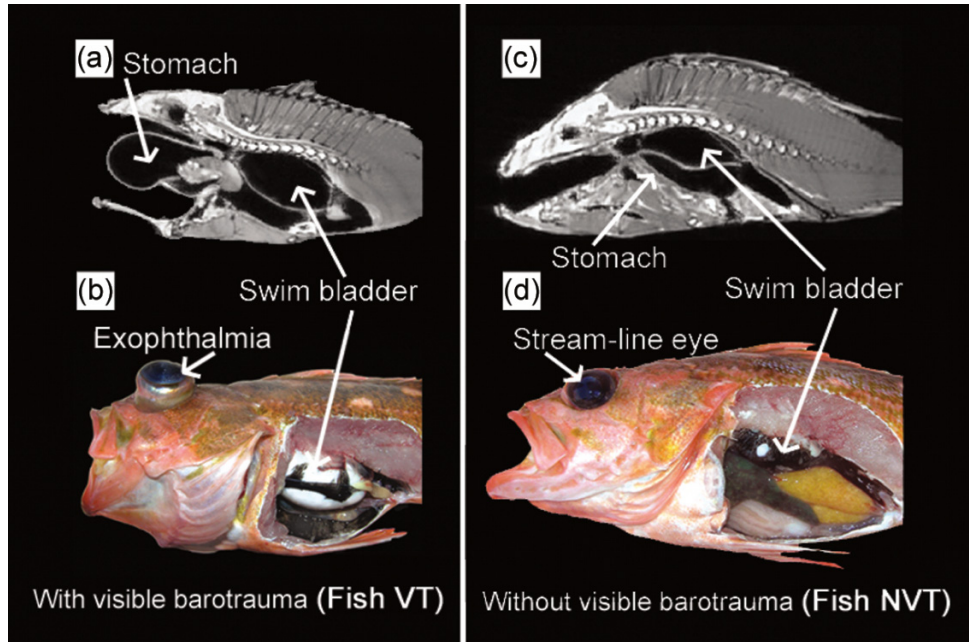
Three-dimensional image segmentation and subsequent volume measurement of anatomical regions were performed using ITK-SNAP v.1.4.1 (Insight Segmentation and Registration Toolkit) (www.itksnap.org/). Segmentation was performed in a semi-automated fashion whereby regions of interest were determined by an expert user who defined points for the full 3D segmentation. A region-growing algorithm was then used to fill out the full organ volume composed of individual known volume units called voxels. MRI image segmentation is always limited by a well-known effect called “partial voluming” that reduces the contrast at tissue boundaries because multiple tissue types inhabit individual voxels.

Both fish were dissected 2 h after scanning to reveal the organ orientation and the orbital eye regions. All external signs of barotrauma remained virtually unchanged from the time of capture to dissection, probably because fish were euthanized with MS-222 and placed in an ice bath during transport to prevent any further major physiological processes from occurring after capture. The swim bladder and internal organs were made visible by cutting away a section of skin and muscle on the left side of each fish (Fig. 1). The eye orbits and optic nerves were made visible by cutting away the frontal cranial bone and clearing away all surrounding tissue. Optic nerve lengths were measured using digital calipers.

Results

Each MRI cross section of the 3D image set was viewed in a separate window, but all sections were analyzed as a whole. Fish VT (male) showed visible stomach eversion to the right side of the buccal cavity up to the buccal edge (Fig. 1). The stomach edges of fish VT were well defined, with a volume of 13.4 cm³, or 9.6% of the whole-fish body volume (Fig. 2). The swim bladder volume of fish VT was

Fig. 1. (a) A sagittal view of one magnetic resonance imaging (MRI) slice showing organ displacement in fish with visible trauma (fish VT) resulting from barotrauma. (b) Photograph of fish VT with dissection window exposing left side of body cavity. (c) Sagittal view of one MRI slice showing less organ displacement in fish with no visible trauma (fish NVT) following rapid decompression. The stomach of fish NVT is small and indistinguishable in this MRI image. (d) Photograph of fish NVT with dissection window exposing left side of body cavity. The swim bladder is covered with dark peritoneum lining and is less visible in this photograph than in (b). A colour version of this figure is available in the Web version of the Journal.



12.2 cm³, or 8.7% of the body. The stomach of fish NVT (female) was 1.4 cm³, or 0.6% of the body (Fig. 2). The swim bladder volume of fish NVT was 10.0 cm³, or 4.1% of the body. When the left sides of each fish were cut away after imaging to reveal internal organs, the internal organs of fish VT were anteriorly displaced, whereas those observed in fish NVT were not (Fig. 2).

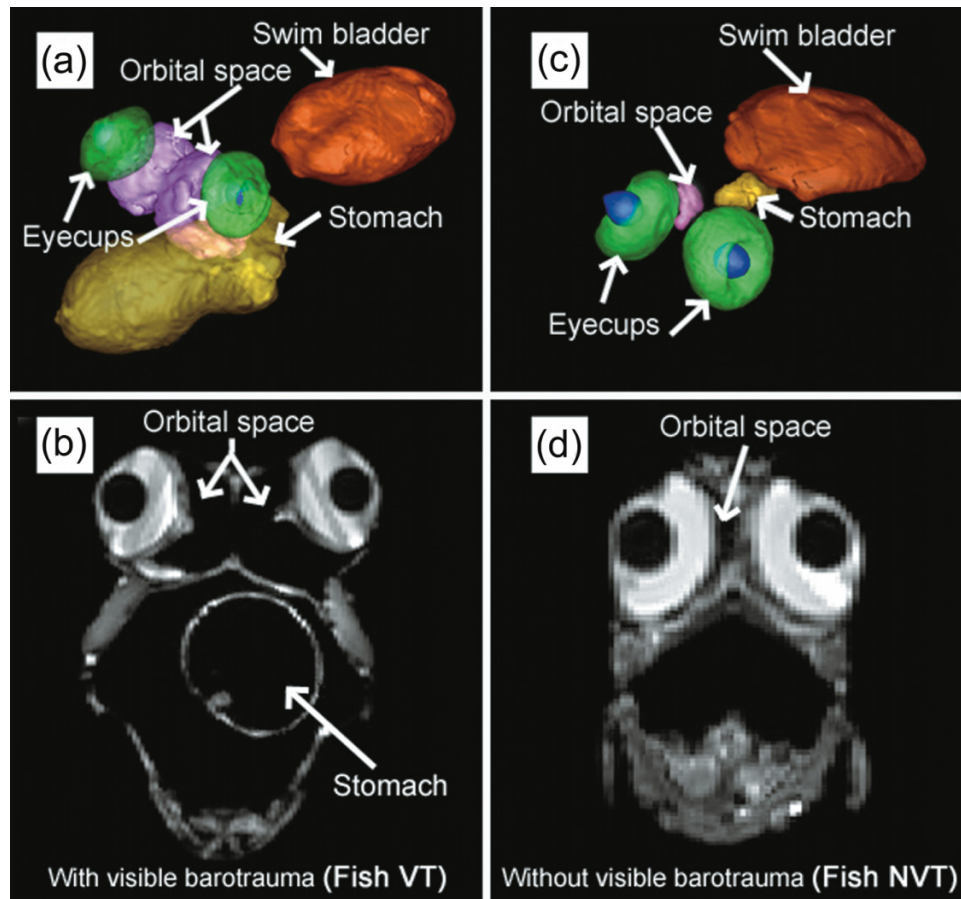
Fish VT showed extreme eye displacement away from its natural medial positioning in the orbital sockets (Fig. 2). MRI images indicate that the eye was physically displaced from the eye socket by subcutaneous gas that formed as an inflated space behind the eye. The volume of this inflated orbital space behind both the right and left eyes combined was 4.9 cm³, or 3.5% of the body volume. The subcutaneous gas volume behind the left eye of fish VT was visibly greater than the gas volume behind the right eye. Additionally, in fish VT, both the optic nerves of each eye and some ocular muscles were stretched when the eye was displaced as a result of the exophthalmia (Fig. 2). Optic nerve lengths measured from dissections for the right and left eyes of fish VT were 10 mm and 9 mm, respectively, and those of fish NVT were 5 mm and 6 mm, respectively. In fish NVT, no orbital space was visible behind the left eye, but a small orbital space behind the right eye occupied 0.05 cm³, or 0.02% of the body (Fig. 2). When all tissues were cleared away around the eyes and optic nerves during dissections, the eyes of fish NVT fell slack away from the orbit as a result of optic nerve stretching. The eyes of fish NVT appeared to be streamline in their natural position and the optic nerves were taut and rigid.

Discussion

The high-resolution 3D images of soft tissue acquired with MRI allow the visual depiction and quantitative assessment of the type and degree of barotrauma, including displacement of the stomach, eyes, and other internal organs, optic nerve stretching, swim bladder overinflation, and the inflation of an orbital space behind the eyes. Because both fish in this study were exposed to barotrauma, future studies should compare rapidly decompressed fish with a control fish that is either caught in shallow water to prevent decompression effects or that has been allowed to fully off-gas the swim bladder during ascent. External signs of barotrauma differed between the two species, even though they occupy the same habitats and have very similar morphological characteristics. Jarvis and Lowe (2008) found that external signs of barotrauma varied equally within and among species. Therefore, the differences in response to barotrauma in our study may not necessarily be due to species-specific characteristics. The fish in this study were of opposite sex, and their varying degrees of barotrauma could possibly be due to sex-related differences. The result of barotrauma in gravid females may change the degree of organ displacement or lead to increased internal compression of organs.

Following rapid decompression, swim bladder gases expand due to a decrease in hydrostatic pressure, and an increase in such volumes can reduce body cavity space available to other internal organs (Rummer and Bennett 2005). Dissection of fish VT revealed an enlarged swim bladder, which displaced the stomach, liver, and other

Fig. 2. (a) A three-dimensional (3D) rendering of the segmented regions in fish with visible trauma (fish VT), showing the eyecups, stomach, swim bladder, and orbital space. Volumes of these regions were estimated based on magnetic resonance imaging (MRI) voxels. (b) Cross-sectional MRI slice of fish VT through the head showing extreme eye displacement. The white protrusions extending off the medial part of the eyes are the optic nerves, which appear short because of their angle relative to this MRI slice. The stomach is prolapsed out the buccal cavity of fish VT. The white circle is the outline of the stomach. (c) A 3D rendering of the segmented regions in fish with no visible trauma (fish NVT). (d) The eyes of fish NVT exhibit more normal placement, where only a small black region depicts a smaller gas-filled orbital space. A colour version of this figure is available in the Web version of the Journal. In the Web version, in parts a and c, the eyes are indicated in green, the lenses in blue, the stomach in yellow, the swim bladder in red, and orbital space in purple.



organs. This could possibly cause organ damage by physically compressing or distorting organs. In the dissection of fish NVT, no displacement of internal organs was observed, despite a low to moderately overinflated swim bladder.

During rapid decompression, expanding gas escaping from the swim bladder likely ruptures the peritoneum and fills the orbital regions, forcing pressure to increase behind the eye and pushing the eye out of its socket. This leads to stretching of the optic nerve and muscles that attach the eye to the brain and skull. Additionally, despite lack of visible external trauma in fish NVT, the MRI images show a small orbital gas-filled space behind the right eye, suggesting that some tissue damage may occur even in fish without visible exophthalmia. However, these smaller pockets of gas that do not result in exophthalmia are less likely to create optic nerve stretching. In dissections, this orbital space could not be seen. Previous research on guinea pigs (*Cavia porcellus*) induced axonal injury to optic nerves by physically pulling the orbital globe out of the eye socket and stretching the optic nerves and then recording abnormalities in optic nerve

cell structure (Maxwell et al. 2003). The highest numbers of damaged axons were found half way along the length of the optic nerve, depicted by dissociation of myelin lamellae and other morphological alterations (Maxwell et al. 2003). Therefore, stretching of the optic nerve in rockfish could lead to nerve damage and possible vision loss.

High-resolution T_2 -weighted MR images of rockfish allowed accurate quantitative assessment of gas-filled spaces in the body, as well as displacement of the swim bladder, stomach, and eyes. Although large organs and spaces were easily segmented, smaller or very complex organ areas such as the lenses, eyes, and whole body were difficult to segment because of the limitations in scanner resolution. Much higher spatial resolution is attainable with higher field MRI scanners and will be important in performing a similar analysis on smaller structures such as the optic nerve, retina, and choroids. Swim bladder overinflation, stomach eversion, and optic nerve stretching were confirmed using dissections, but the orbital space was not visible in dissections. Segmenting body regions in rockfish can prove useful for analyzing

morphological damage or inflation of organs and regions in rockfish specimens following barotrauma and assessing the level of damage quantitatively, without disrupting the structural integrity of gas-filled spaces or the fish as a whole. Furthermore, our study provides pertinent information on individuals of economically important groundfish populations and provides a unique method for making barotrauma-associated comparisons across all rockfish species.

Acknowledgements

Support for this research was provided in part by the University of Southern California Sea Grant College Program of NOAA under grant No. NA06OAR4170012 and the State of California Resources Agency, and in part by the Minerals Management Service under cooperative agreement No. 1435-01-04-CA-34196 (C.G.L.), the Digital Fish Library, and the National Science Foundation (No. DBI-0446389 to L.R.F. and No. DBI-0641550 to E.F.J.).

References

- Davis, M. 2002. Key principles for understanding fish bycatch discard mortality. *Can. J. Fish. Aquat. Sci.* **59**: 1834–1843. doi:10.1139/f02-139.
- Hannah, R.W., and Matteson, K.M. 2007. Behavior of nine species of Pacific rockfish after hook-and-line capture, recompression, and release. *Trans. Am. Fish. Soc.* **136**: 24–33. doi:10.1577/T06-022.1.
- Jarvis, E., and Lowe, C.G. 2008. The effects of barotrauma on the catch-and-release survival of southern California nearshore and shelf rockfish (Sebastidae, *Sebastes* spp.). *Can. J. Fish. Aquat. Sci.* **65**: 1286–1296. doi:10.1139/F08-071.
- Love, M.S., Yoklavich, M., and Thorsteinson, L. 2002. *Rockfishes of the Northeast Pacific*. University of California Press, Berkeley, California.
- Maxwell, W.L., Domleo, A., McColl, G., Jafari, S.S., and Graham, D.I. 2003. Post-acute alterations in the axonal cytoskeleton after traumatic axonal injury. *J. Neurotrauma*, **20**: 151–168. doi:10.1089/08977150360547071. PMID:12675969.
- Nichol, D.G., and Chilton, E.A. 2006. Recuperation and behaviour of Pacific cod after barotrauma. *ICES J. Mar. Sci.* **63**: 83–94. doi:10.1016/j.icesjms.2005.05.021.
- Parker, S.J., McElderry, H.I., Rankin, P.S., and Hannah, R.W. 2006. Buoyancy regulation and barotrauma in two species of nearshore rockfish. *Trans. Am. Fish. Soc.* **135**: 1213–1223. doi:10.1577/T06-014.1.
- Perry, C.N., Cartamil, D.P., Bernal, D., Sepulveda, C.A., Theilmann, R.J., Graham, J.B., and Frank, L.R. 2007. Quantification of red myotomal muscle volume and geometry in the shortfin mako shark (*Isurus oxyrinchus*) and the salmon shark (*Lamna ditropis*) using T_1 -weighted magnetic resonance imaging. *J. Morphol.* **268**: 284–292. doi:10.1002/jmor.10516. PMID:17299779.
- Rummer, J.L., and Bennett, W.A. 2005. Physiological effects of swim bladder overexpansion and catastrophic decompression on red snapper. *Trans. Am. Fish. Soc.* **134**: 1457–1470. doi:10.1577/T04-235.1.
- Wilson, R.R., Jr., and Burns, K.M. 1996. Potential survival of released groupers caught deeper than 40 m based on shipboard and in-situ observations, and tag-recapture data. *Bull. Mar. Sci.* **58**: 234–247.